

Fig. 14: Part of the pattern file for learning Neural Network. All the datas come from experimental testings and some interpolations are made numerically by FEA on the presented model.

5. CONCLUSION REMARK

1. Although cold-drawn smooth bars are also declared for possible use in glued-in bolted connections, this paper with its results emphasize the dangerousness of using it. Adhesion between smooth steel bars and glue is questionable. There is also possibility of loosing strength due to corrosion of the steel bar. as could be seen from the experiments, smooth steel bars just slips trough glue. Ultimate axial force (see Fig. 10) is significantly smaller than characteristic axial capacity in tension suggested by Riberholt (1988) :

$$R_{ax,k} = f_{ws} \cdot \rho_k \cdot d \cdot \sqrt{l_g}, \quad \text{where } f_{w,s} \text{ is strength parametar. For brittle glues such as epoxy the value is 0.52}$$

and about the same or smaller then characteristic axial capacity in tension suggested by Eurocode 5-Part2-Appendix A:

$$F_{ax, Rk} = \pi \cdot d_{equ} \cdot l_a \cdot f_{v, k}$$

It is of course logical to use rebars or threaded bars but somebody less informed must be warned that smooth steel bars are not allowed to be used in glued-in bolts joints. Or their axial tension strength capacity should be reduced.

2. From the diagrams (see Fig. 7-10.) it could be seen that the axial strength is somewhat higher for bolts glued-in perpendicular to grain direction.

3. The glued-in bolts joints should be used with lots of extra care, because during the experiments some of the results are significantly fail regarding axial strength capacity witout mistakes in production.

4. Neural network could be very good tool in prediction strength capacity of the glued-in bolts because it can contains much more datas which are valuable such as temperature in glue or in wood, moisture in both materials, production method, properties of various kind of glue.

5. REFERENCES

1. Bodig, J., Jayne, B.A. (1982): Mechanics of wood and wood composites. Van Nostrand Reinhold, New York, USA
2. Aicher, S., Herr, J. (1998.): Investigations on high strength glulam frame corners with glued-in steel connectors, Proceedings of 5th WCTE, Montreux, Switzerland, Vol 1.
3. Aicher, S (1992.): Testing of Adhesives for Bonded Wood-Steel Joints, Proceedings of the Meeting IUFRO S 5.02, Bordeaux, France.
4. COSMOS 2.5 (2000.): Reference Guide, Vol1-Vol4, SRAC, USA
5. Rajčić, V., Bjelanović, A., Rak, M. (2004): Experimental Test of Glued in Bolt Joint using Threaded Steel Bars, Proceedings of 8th WCTE, Lahti, Finland, 317-320.
6. NeuroShell 2, Ward System, Reference Guide, USA.

Therefore, any potential user of trained NN, should be at least briefly informed (by NN) about joint strength capacity. Further researches into the scope of application of NN might be direct to provide the appropriate equation for describing the behaviour of this type of joint and predicting of their strength. Trained NN might be helpful in it because of its capability of "fitting" through dates.

Also, there is a big influence of the moisture content and change of it and temperature condition that influence glue as well as wood. That influence was not predicted in design rules for axially loaded glued-in and laterally loaded bolts given in Eurocode 5-Part 2-Appendix A and could be nicely foreseen using Neural Network results of learning.

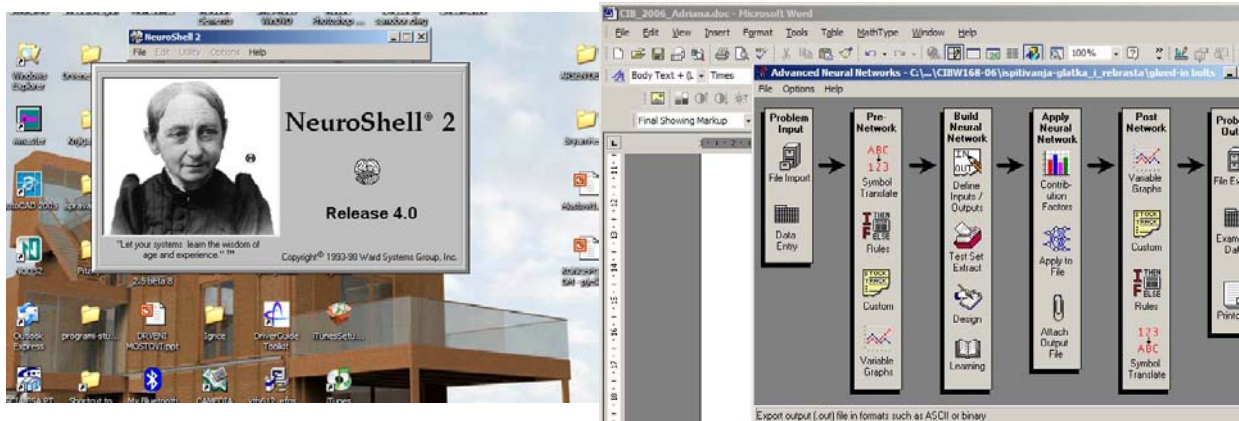


Fig. 13: Neural Network shell NeuroShell 2 was used for "training" the problem of the axial tension capacity of the glued-in bolts. Menu of the neural network shell is presented. Advanced learning with back propagation algorithm was used.

Datagrid: C:\... \clanci\CIBW168-06\ispitivanja-glatka_i_rebrasta\uljenesopke.pat

File Edit Format Help

Number of row with variable names (blank if none): 1 left/right arrow keys end edit

First row containing actual training data: 2 Size: 179 row 20 columns

Note: This is not a commercial spreadsheet and may not load fast enough for large files. The NeuroShell 2 Options menu allows you to change the datagrid call to your own spreadsheet. Search help file for "datagrid" for details.

	A	B	C	D	E	F	G	
1	width of specimen	moisture	effective diameter	glued length of bolt	fract. tensile force (kN)	normal stress sx	perpendicular stress sy	shear
2	20,0000000000	10,9000000000	16,0000000000	80,0000000000	14,0800000000	7,7000000000	0,5700000000	
3	20,0000000000	12,3000000000	16,0000000000	80,0000000000	13,0400000000	6,8000000000	0,5700000000	
4	20,1000000000	10,7000000000	16,0000000000	80,0000000000	14,0500000000	7,2000000000	0,5600000000	
5	20,0000000000	11,3000000000	16,0000000000	80,0000000000	15,0400000000	7,2000000000	0,5400000000	
6	20,0000000000	11,2000000000	16,0000000000	80,0000000000	14,9500000000	6,8000000000	0,4300000000	
7	20,0000000000	10,9000000000	16,0000000000	80,0000000000	13,9100000000	7,1000000000	0,5600000000	
8	20,2000000000	10,6000000000	16,0000000000	80,0000000000	14,5500000000	5,9000000000	0,4500000000	
9	20,1000000000	10,4000000000	16,0000000000	80,0000000000	13,7000000000	6,1000000000	0,4200000000	
10	20,0000000000	11,9000000000	16,0000000000	80,0000000000	14,7500000000	6,7500000000	0,4400000000	
11	20,0500000000	10,5000000000	16,0000000000	80,0000000000	13,8000000000	6,9000000000	0,4600000000	
12	20,0000000000	11,7000000000	16,0000000000	80,0000000000	14,1300000000	7,2000000000	0,5700000000	
13	20,2000000000	11,4000000000	16,0000000000	80,0000000000	14,3000000000	5,8600000000	0,4500000000	
14	20,1000000000	10,2000000000	12,0000000000	80,0000000000	14,0300000000	5,9400000000	0,5500000000	
15	20,0500000000	9,9000000000	12,0000000000	80,0000000000	13,7500000000	6,1200000000	0,4600000000	
16	20,0300000000	10,3500000000	12,0000000000	120,0000000000	18,5100000000	5,9200000000	0,4500000000	
17	20,0500000000	11,2000000000	12,0000000000	120,0000000000	17,8800000000	7,0000000000	0,5400000000	
18	20,0000000000	10,3300000000	12,0000000000	120,0000000000	19,6300000000	7,4000000000	0,4400000000	
19	20,0300000000	12,1000000000	12,0000000000	120,0000000000	17,8800000000	7,5000000000	0,5400000000	
20	20,0000000000	11,0000000000	12,0000000000	120,0000000000	18,3600000000	6,4000000000	0,4900000000	
21	20,0800000000	10,4000000000	12,0000000000	120,0000000000	18,0100000000	7,2000000000	0,5800000000	
22	20,0000000000	11,1000000000	12,0000000000	120,0000000000	17,6500000000	6,8500000000	0,5800000000	
23	16,0200000000	12,1000000000	12,0000000000	120,0000000000	18,9100000000	7,1200000000	0,5800000000	
24	16,0000000000	9,8000000000	12,0000000000	120,0000000000	17,6700000000	6,9900000000	0,4400000000	
25	16,0600000000	11,2000000000	16,0000000000	120,0000000000	21,5500000000	5,8800000000	0,5700000000	
26	20,0600000000	10,3000000000	16,0000000000	120,0000000000	22,4600000000	6,7500000000	0,4100000000	
27	16,0300000000	11,1500000000	16,0000000000	120,0000000000	22,1300000000	7,0050000000	0,5800000000	
28	16,0500000000	10,6500000000	16,0000000000	120,0000000000	21,7800000000	6,9800000000	0,5800000000	
29	16,1000000000	11,3500000000	16,0000000000	120,0000000000	21,9500000000	7,2000000000	0,5200000000	
30	16,0000000000	11,4000000000	16,0000000000	120,0000000000	23,0100000000	6,8800000000	0,5400000000	
31	16,0400000000	10,2000000000	16,0000000000	120,0000000000	22,0800000000	5,8800000000	0,5800000000	
32	16,0300000000	10,7500000000	16,0000000000	120,0000000000	21,8600000000	6,1200000000	0,4800000000	
33	16,0700000000	11,2500000000	16,0000000000	120,0000000000	22,1000000000	5,2100000000	0,5000000000	
34	16,3000000000	10,2000000000	16,0000000000	120,0000000000	22,4000000000	6,1200000000	0,5700000000	
35	16,0600000000	11,6700000000	16,0000000000	120,0000000000	21,1100000000	6,0000000000	0,5900000000	
36	16,0700000000	11,1000000000	16,0000000000	120,0000000000	21,9600000000	7,0000000000	0,5100000000	

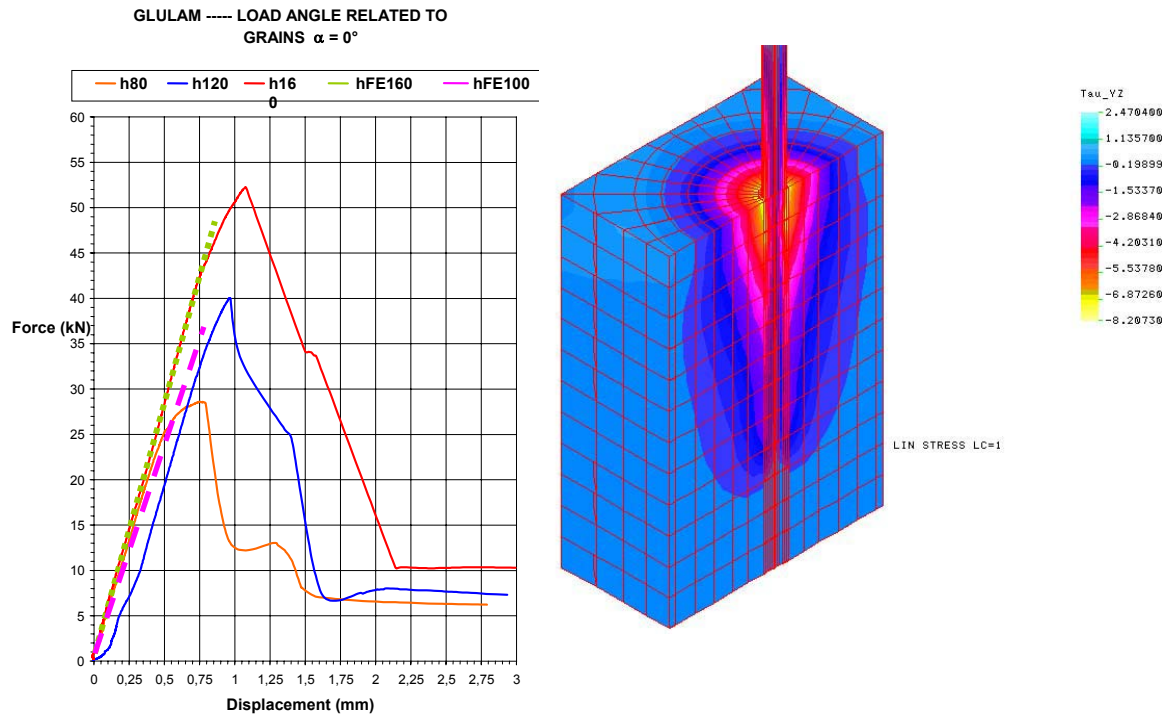


Fig. 12: Comparison of results obtain experimentally and numerically for load 0° -angle Strength failure type for load 0° -angle – shear stresses measured on fracture area

4. NEURAL NETWORK AS AN AUXILIARY TECHNIQUES FOR JOINT STRENGTH CAPACITY PREDICTION

The four Neural Network models (one for an each load angle related to wood fibers and one for an each type of glued-in steel bars) on the set pattern of an average number of fifty different cases per each NN model. Inputs had been separated as they follow: the width of the cross-section of specimens (A), the depth of the cross-section of specimens (B), the depth of specimens (HD), the diameter of threaded steel bars (D), the load angle (AL) and the depth of an anchorage of threaded steel bars (H), as well. The value of the tensional force of fracture (P) was the first output parameter. We have found that stress and deformation values, as well, significant for an each mode of strength failure, were the logical output values. They are as they follow: the shear stresses (TYZ) and normal stresses (SX, SY) as well) and the displacement measured on the contact line lay between the wood and the glue (for threaded bars) or between bar and glue (for cold-drawn smooth steel bars), as well as the displacement of the upper grain of the specimen.

We used the Back Propagation algorithm of Standard Connection and supervised learning for an each generated model of Neural Network. The learning was interrupted after approximately two hours, when the average error of test patterns reached value less than 0.25%. The successful completion of NN training was achieved when NN models had been claimed to produce results of their own based on, until, unseen inputs. When we have compared results produced by NN with expected values (by FE linear analysis of numerical models), it was clear that they correlate very well. Maximum deviation between them did not exceed 1.5–2.0%, and average values were less than the mentioned one.

in the same way. Mechanical characteristics of an anisotropic GluLam Fir was defined in local coordinate system where a local x-axis always lies parallel with fibers direction (see Table 1 and Table 2). It is clear that the anchorage depth and the diameter of rods, glue fracture energy and loading conditions are decisive for expression of the mean shear stress at the failure. For small anchorage depths, like those we experimented with, the load is almost proportional with shear failure stress, so, we used only linear FE analysis to determine the failure stress values.

Comparison of results of experimental tests with results of analysis of 3D FE models was the next step of carried out researching. Numerical FE analysis is based on linear fracture mechanics analysis of the model of the adhesive layer's behaviour. Satisfactory correlation between experimentally and numerically obtained results was an ultimate issue we intended to achieve. During the linear analysis of FE models the following parameters had been varied (see Fig.11): the geometry of the model, the diameter of the bars, an anchorage depth of glued-in rods and the load angle in comparison with wooden fibers (0° and 90°). The thickness of the glue to fill provided holes was kept constant (1,5mm).

The decisive thesis that we tried to verify and to proof is: if we could find the validity of relationship between results obtained experimentally and numerically, then, we can dominantly use numerical model to continue researching and to explore an influence on joint strength capacity caused by variation of diameters and anchorage depths of steel bars (see Fig.12).

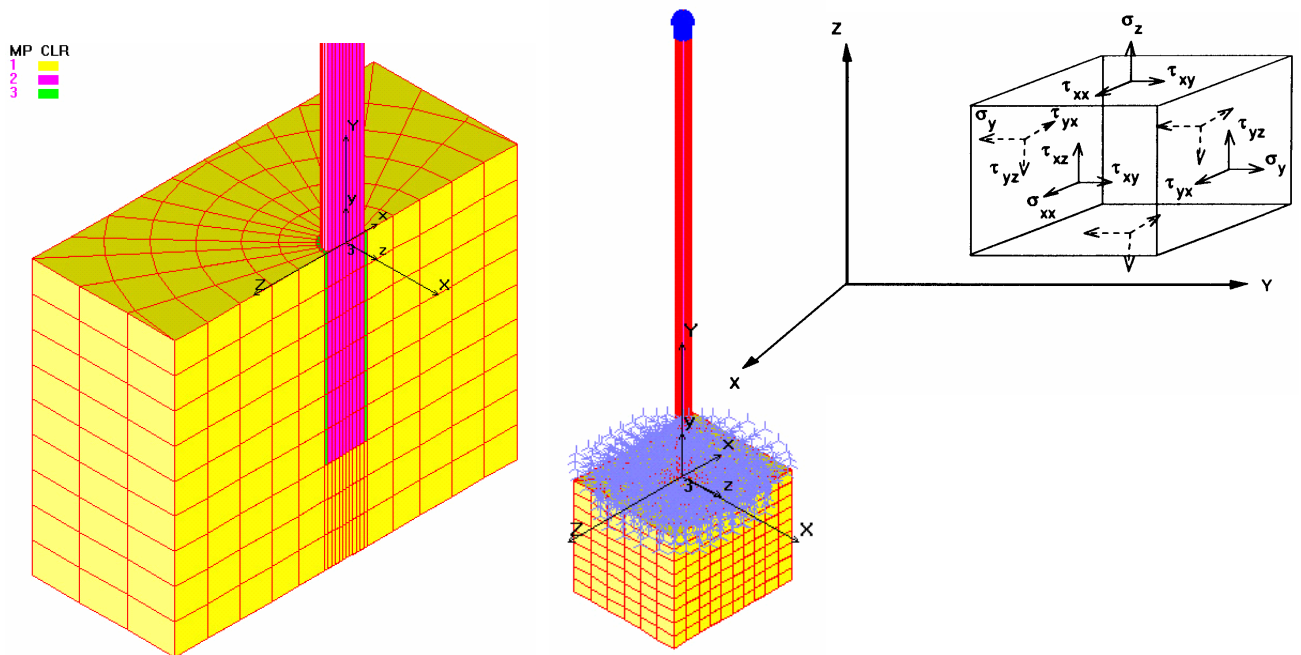


Fig. 11: Example of one FE 3D parametrically prepared model (geometrical parameters for 90° -load angle together with material property definition and the directions of stress components outputs for SOLID FE)

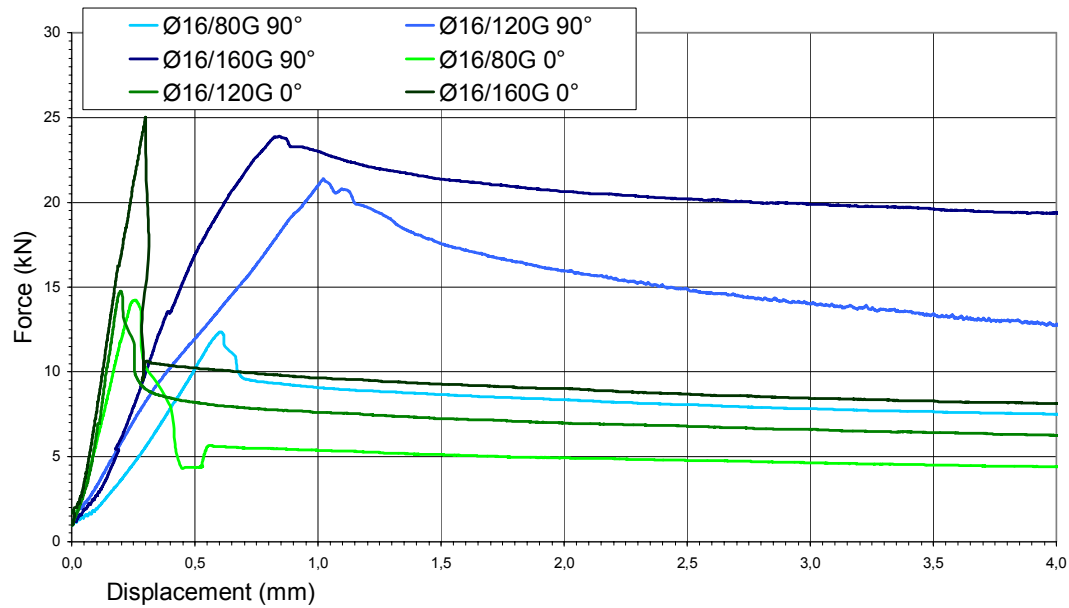


Fig. 9: Experimental results for cold-drawn steel bars of $d = 16\text{mm}$ and EPOCON glue: F - d diagrams for various load angles and anchorage depths (H)

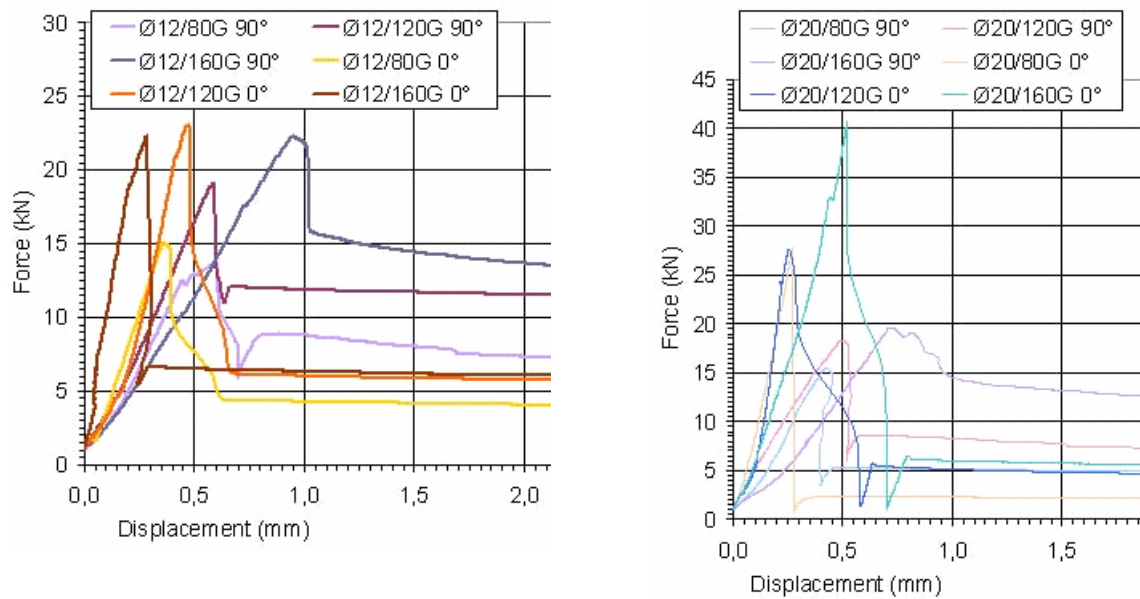


Fig. 10: Experimental results for cold-drawn bars of $d = 12(20)\text{ mm}$ and EPOCON glue: F - D diagrams for various load angles and anchorage depths (H)

3. NUMERICAL FE ANALYSIS

COSMOS /M programme was used for numerical analysis where only SOLID finite elements were constitutive part of an each 3D parametrically prepared model. SOLID is an 8-node three-dimensional where three translation degrees of freedom per node are considered for structural analysis. The direction of output stress components was defined

medium values of the F–d relationship have been collected to represent the joint fracture behaviour during the tests.

It is clear that the anchorage depth (H), and loading conditions, the glue type as well as the bar type (threaded or cold-drawn smooth steel bars) are decisive for expression of the mean shear stress at the failure. We have found that the higher joint strength capacity for both glue types and for threaded bars was reached for the load angle of $\alpha = 90^\circ$ (see Fig. 5, Fig. 6 and Fig. 7). The failure force reached insignificantly higher values in tests where the EPOCON glue was used but this difference (related to SIKADUR bond) did not exceed approximately 10% of the measured failure value.

Significantly lower joint strength capacity was achieved for cold-drawn smooth steel bar (see Fig. 8 and Fig. 9) where the failure takes place in the glue, along the smooth surface of the cold-drawn smooth steel bar. We have also found that previously described failure type was characteristics for both load angles (of 0° and 90° , see Fig. 8 – 10) which means that the failure behaviour is very independent of load angle – fiber direction relation. Unfortunately, in spite of cold-drawn steel bars, we did not make test for both glue types (those were carried out only for EPOCON), so, we could not compare results and accomplish some conclusions in this field. However, it is obviously that a slipping along the smooth surface of a steel bar (placed between the bar and the glue) is predominance for the fracture behaviour. Slipping module is much higher for this type of steel bars (in comparison with threaded steel rods).

Also, there are no reliable proofs neither for the durability of adhesion of cold-drawn smooth steel bars nor for the influence of their corrosion. Facts we have just mentioned, together with results which experiments carried out, do not speak in favor of smooth steel bars if we try to compare them with threaded rods (see Fig. 5 to Fig. 10).

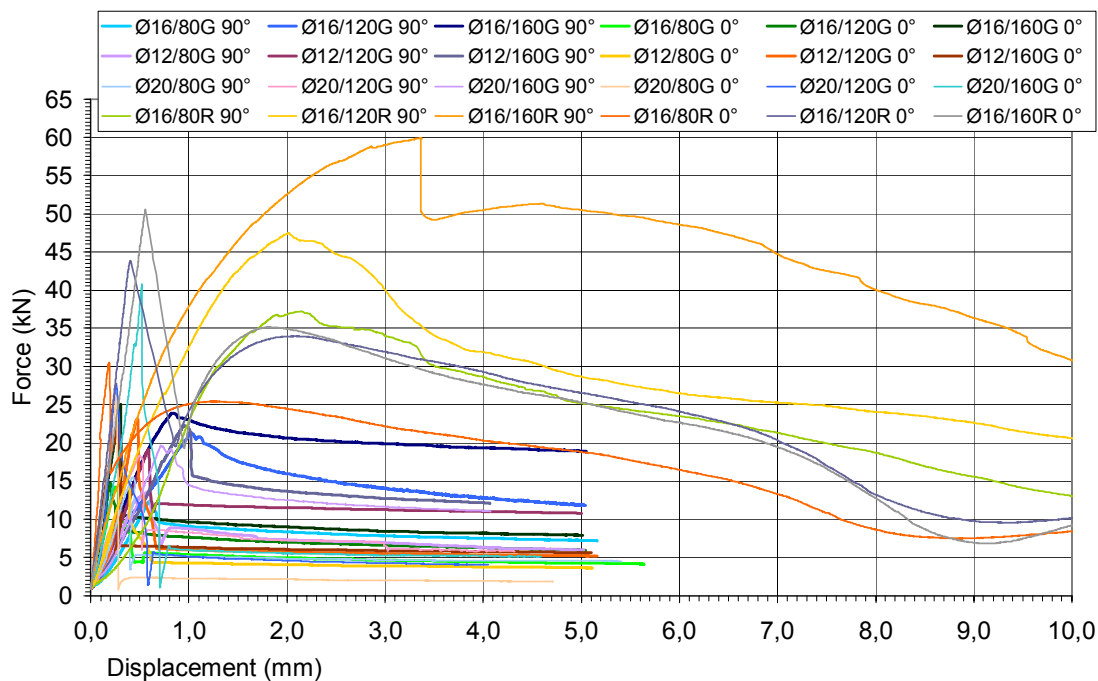


Fig. 8: Collected test results for both steel bars type and for the EPOCON glue: F–D diagrams for various load angles (α), diameters (d) and anchorage depths (H), (G)- smooth cold-drawn steel bars

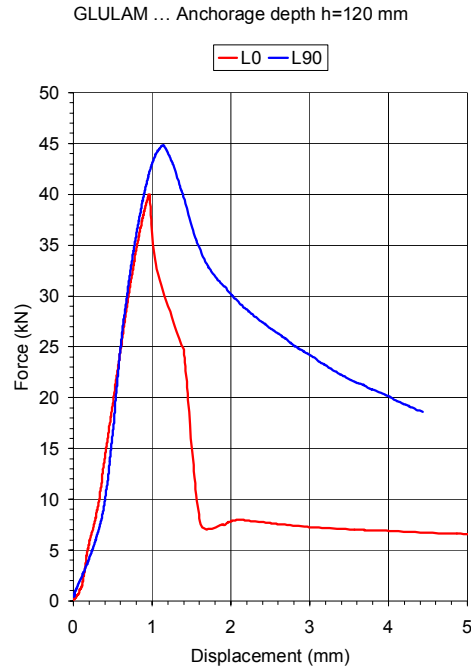


Fig. 6: Comparison of experimental results ($F - d$) for threaded steel bars ($d = 16\text{mm}$), SIKADUR glue and anchorage depth of $h = 120\text{mm}$ due to load angle

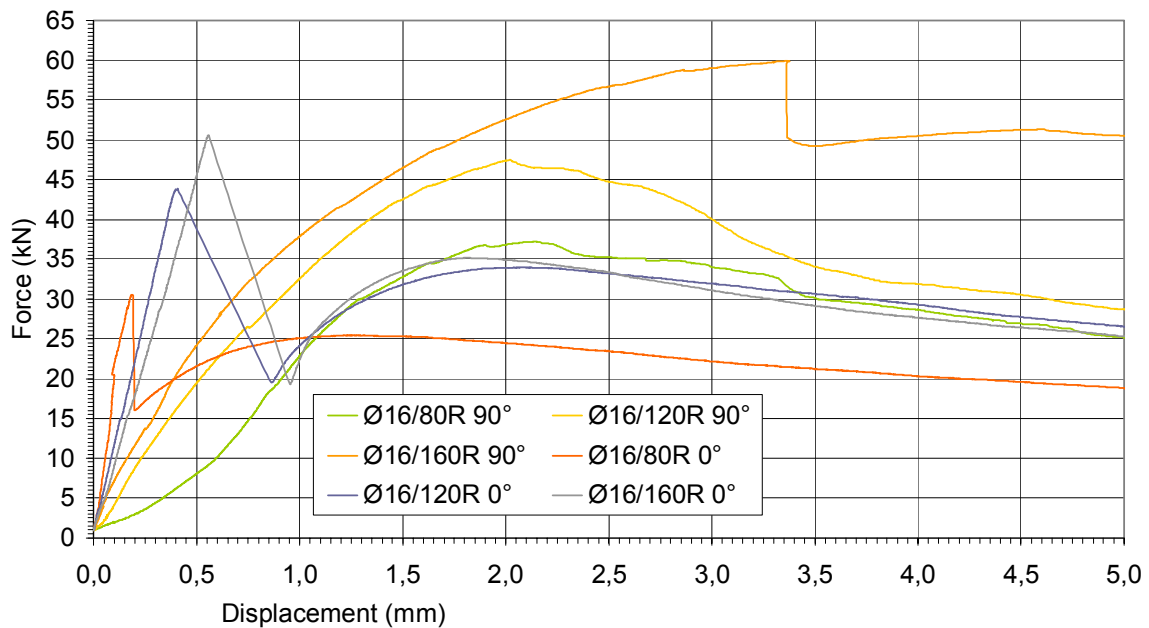
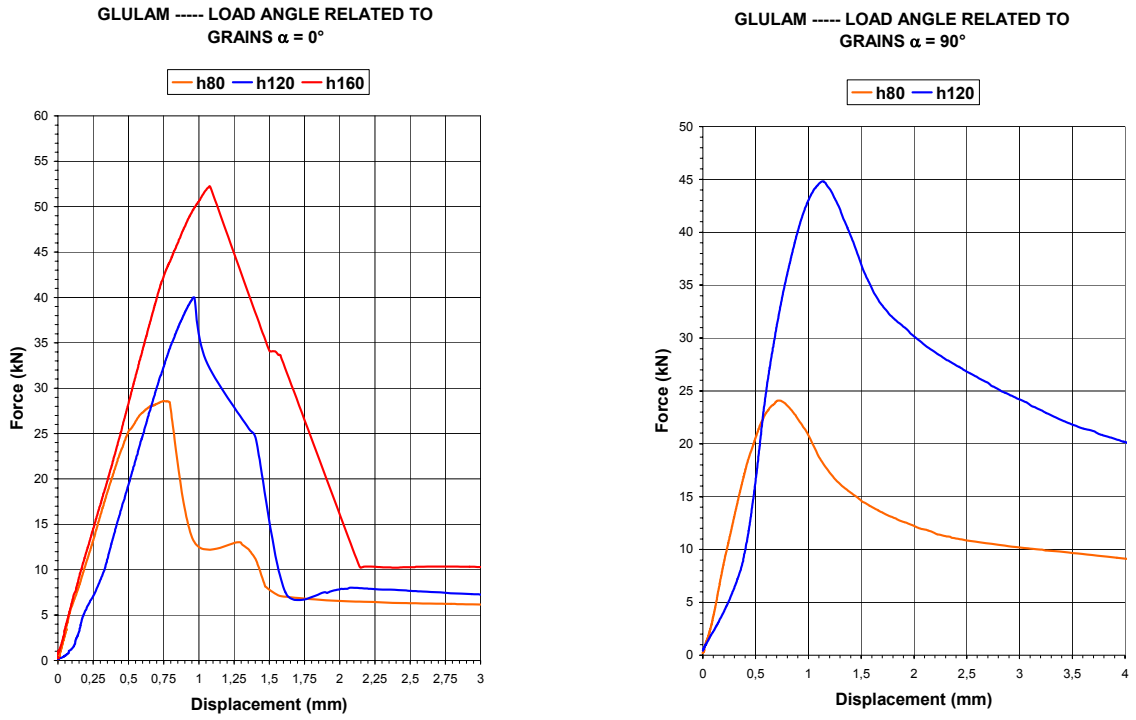


Fig. 7: Experimental results for steel rebars ($d = 16\text{mm}$) and EPOCON glue: $F - D$ diagram for various load angles (α) and anchorage depths (H), R-rebar

Laboratory made one-side pull-out tests carried out the $F - d$ diagram for an each specimen. A force increase was provoked by constant deformation increase. The connection involves possibility of plasticity, as it is apparent that after the elastic deformation and, upon reaching the failure strength of the cross section, there is a further strength possibility up to a certain level (see Fig. 5 – Fig. 6). Measuring results of all

strength capacity is characteristic by failure along the glue, which is typical for 90° – tests (see Fig. 4 – 7).

2.2. Experimentally Determined Joint Strength Failure



(a) Test Load Angle $\alpha = 0^\circ$

(b) Test Load Angle $\alpha = 90^\circ$

Fig. 5: Experimental results for threaded steel bars ($d = 16\text{mm}$) and SIKADUR glue: F - d diagram for various load angles (α) and anchorage depths (H)



Fig 3: Setting up of experiments with EPOCON 88 glue



Fig. 4: The two basic types of fracture behaviour for joints with threaded bars due to load angle related to fibers

The first failure type is characteristic for 0° – tests (see Fig. 4 – 7) and threaded steel bars glued-in. The failure takes place in the wood along irregular surface, a few millimetres along the threaded bar, where there are the highest stress values. The second type of joint

Table 1: Measured material properties and moisture percentage of GluLam Fir specimens in [MPa]

$E_{0,mean} = 11700$	$\nu = 0,303$	$f_{v,0,FAILURE} = 8,33$	$u = 10\%$
----------------------	---------------	--------------------------	------------

Table 2: Material properties of steel bars and measured values in [MPa] for both epoxy two-component glues (SIKADUR 31 RAPID, EPOCON 88 KGK)

Steel material and epoxy glues	E-module	G-module	Poisson
Steel 235	210000	81000	0,27
SIKADUR 31 RAPID	4120	1420	0,45
EPOCON 88 KGK	7200	2170	0,336

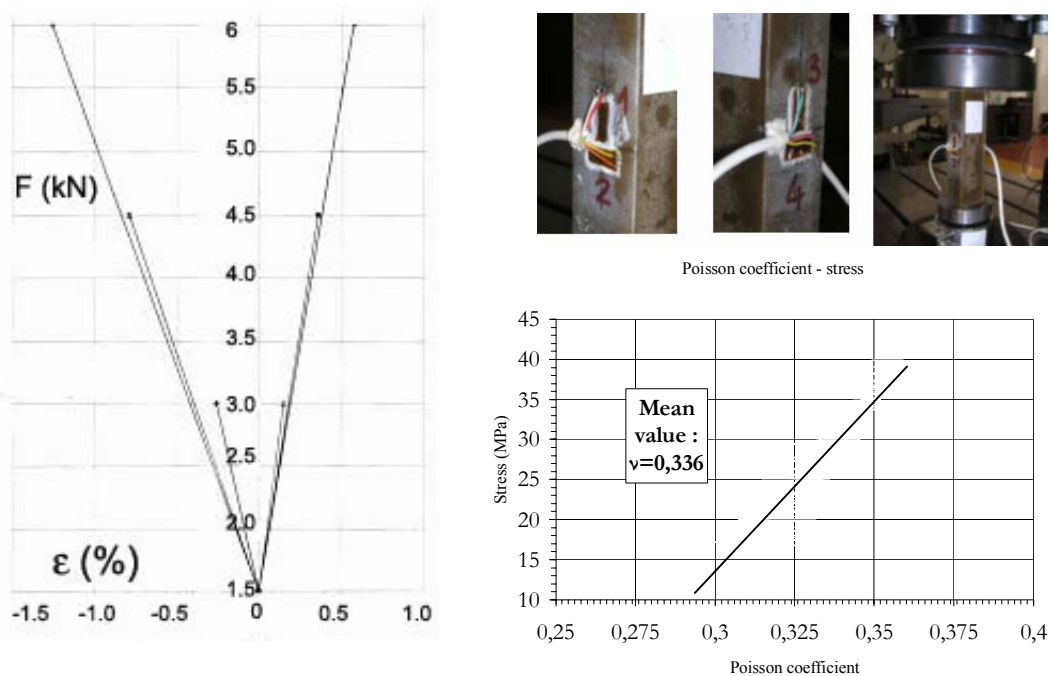


Fig 2: $F - \varepsilon$ diagrams or SIKADUR 31 RAPID (left) and EPOCON 88 KGK (right) glues

The experiments to obtain axial tension strength of glued in smooth cold-drawn bars and rebars glued with EPOCON 88 were done by test machine system Zwick which can satisfy demands and performs superior test tasks. The tests were driven by the rule of the constant increase of the deformation. Software *testExpert* was used for data analysis and statistics. The digital technology drive system features a high control range. The lower extensometers were placed on the top level of the wooden sample and the higher extensometers are placed on the steel bars. The measured displacement between wood sample and bar was difference between the results from two level extensometers. The result are given as the F-d diagrams.

2. EXPERIMENTAL RESEARCHING

2.1. Specimens and material properties

The laboratory tests were performed by one-side destructive pull-out test [1]. Each of four classified groups of specimens was characterised by different anchorage angle of bars (related to grains): 0° and 90° (see Fig.1), as well as by different glue type. Specimens were undergone to laboratory testing of their material properties (see Tab. 1), as well as glues were (see Tab. 2). The diameter of tested steel bars was varied for all specimens ($d = 12\text{mm}$, 16mm and 20mm). A hollow steel plate laid on the specimens of different shapes to prevent all possible displacements as well as to transfer a compressive load onto specimen over itself. All displacements were prevented in the zone of the steel plate on the parametrically prepared 3D models. A compressive load is transferred over the plate onto the specimen, and the bar is pulled out on the opposite side.

We varied an anchorage depth of bars (80mm , 120mm and 160mm), but the thickness of both types (two – component) epoxy glues to fill provided holes was kept constant ($1,5\text{mm}$).

Each of the four groups consists of approximately ten specimens with different anchorage depth

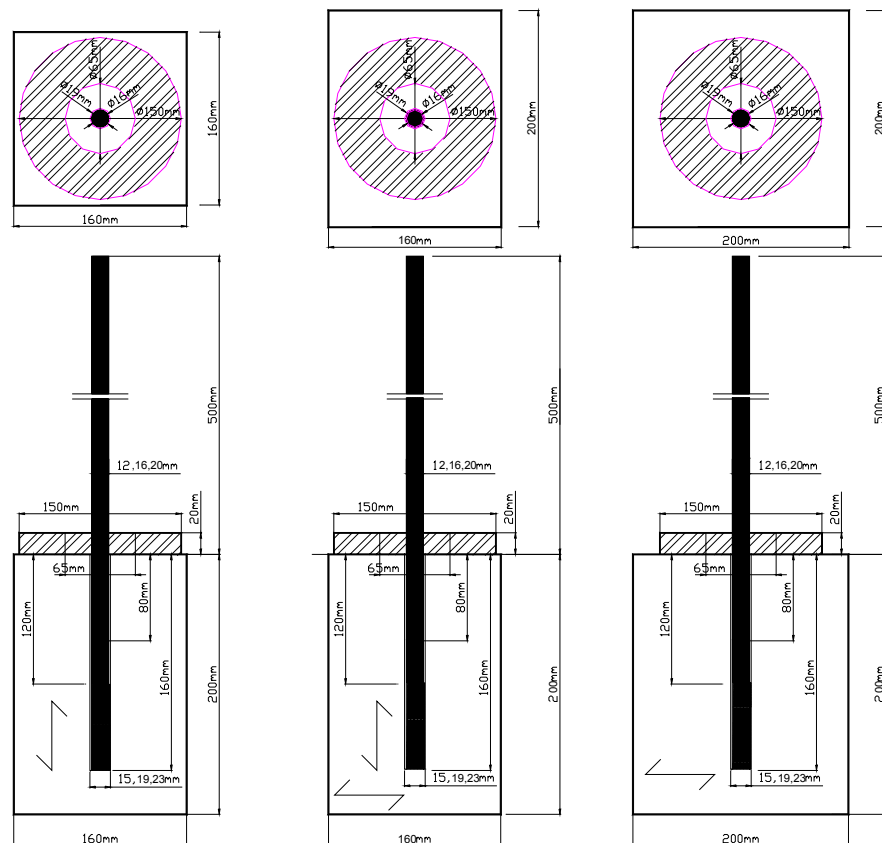


Fig 1: Shapes of tested groups of specimens with load angle of 0° and 90°

The threaded steel bars were manually embedded into the holes under constant pressure and rotation. The centring of the bars during embedding was visually performed.

Comparison of the Pull-out Strength of Steel Bars Glued in GluLam Elements Obtained Experimentally and Numerically

Vlatka Rajcic, Adriana Bjelanovic, Mladenko Rak

Prof, PhD, str. eng., Assist. Prof, PhD, str. eng., Prof, PhD, str. eng., Croatia

1. Introduction

The paper presents the comparison of results obtained experimentally and numerically as well as the efficiency of trained Neural Network in prediction of the strength capacity of the bolted joints made with bars of cold-drawn smooth steel and threaded steel bars glued-in in GluLam elements. Joint specimens were undergone to destructive one-side pull-out test. The experiment was the starting point of the whole process with purpose of determining the tensile strength of joint. The whole research work and comparison of the experimentally obtained results have been made of several different levels and goals. The first one focused on fracture behaviour of joints made of cold-drawn smooth and threaded bars using the same adhesive layer, EPOCON 88 KGK. The second comparison level was focused on fracture behaviour of joints made of threaded bars while different species of bond layer was used SIKADUR 31 RAPID and EPOCON 88. The third level of research based on comparison of experimental and numerical results for joints bolted with threaded bars only where the results of 3D parametrically prepared models undergone to linear FE analysis in COSMOS/M program. Satisfactory correlation between experimentally obtained results and those that numerically produced was an ultimate issue that been intended to achieve.

Results of FE linear analysis obtained on 3D numerical models used for generating of NN database. The decisive thesis we try to verify was: if we could find the validity of relationship between results obtained experimentally and numerically, then we can use only numerical model to continue researching and make it extensively. We can use then only numerical FE model to explore an influence on joint strength capacity caused by variation of diameters, load angle and anchorage depths of threaded bars, as well.

We also try to make a move over and use results of the FE analysis to generate Neural Network databases. Why Neural Network? The most important fact is that inputs and outputs of FE analysis were recognisable for generated Neural Networks that we trained on them. The whole set of data inputs and outputs have been selected to represent a brief geometrical description of the joint as well as its state of load bearing capacity. The successful completion of an attempt have been achieved when trained NN models produced results of their own, based on, until then, unseen inputs. The interesting thing is correlation of the axial strength obtained by experiments, Neural network prediction strength and design rules suggested for characteristic axial capacity in tension given by Eurocode 5-Part 2-Appendix A.